Design Implications for Local Linear Approximation of Dynamical Physiological Systems Data

Charlotte Clapham

Department of Biostatistics, Johns Hopkins Bloomberg School of Public Health, Baltimore MD, USA

email: cclapha1@jhu.edu

and

Karen Bandeen-Roche

Department of Biostatistics, Johns Hopkins Bloomberg School of Public Health, Baltimore MD, USA

email: kbandee1@jhu.edu

SUMMARY: Physical resilience is a pressing research area in aging. The Study of Physical Resilience and Aging (SPRING) posits that resilience is rooted in the fitness of specific physiological systems: It is studying resilience by introducing stressors on selected systems and monitoring their return to homeostasis as time series. This paper aims to study design properties for such "dynamical systems" data. We modeled post-stressor activity of a theoretical biological system using damped linear oscillators representing varying levels of resilience. We then sampled points from the curves in scenarios varying sparsity of serial observations ("points") and measurement error variance. Local Linear Approximation was used to estimate differential equations characterizing curve dynamics, and accuracy and precision were assessed. Error variability was more impactful than sampling sparsity in curve recovery: With high variability, estimation was biased for all curves regardless of numbers of points sampled. With low variability, curve recovery was possible with few points, and accuracy increased sharply with initial increases in points sampled. Findings inform analytic interpretation and future study design.

KEY WORDS: Dynamical systems modeling; Local linear approximation; Physical resilience; Sparse data

This paper has been submitted for consideration for publication in *Biometrics*

1. Introduction

As the American population ages, physical resilience in older adults is a robust and pressing area of research. Physical resilience reflects how well bodies respond to stressors– how quickly and to what extent systems can bounce back from change. (Hadley et al., 2018). One particularly important category of stressors is that of medical procedures, which become increasingly important and complex as bodies age. Understanding resilience in this setting is crucial in assessing both the impact and necessity of different medical procedures, which would allow providers to make more informed healthcare decisions.

A key way to study resilience is through monitoring how different physiological systems hypothesized to underlie resilience capacity respond to stressors. Considering the relevant physiology as a dynamical system—that responds to provocation according to mechanisms governed by differential equations—may provide a further useful lens for studying resilience. Through this lens, the optimal study design is then to provoke the system in the laboratory or clinic, and examine how it responds. Cortisol levels and glucose levels are two examples of observable markers of such dynamical systems. The amounts of these hormones, chemicals, etc. change in response to stressors and then attempt return to homeostasis, that is, steady state.

It is thought that people with higher resilience return to homeostasis more quickly and successfully than those with lower resilience—whether from a controlled, "laboratory" stressor or a major life stressor such as surgery (Walston et al., 2023). Patterns of physiologic system response post-stressor can be represented with models that reflect the governing equations of the biological process mechanisms. People with low resilience are hypothesized to have different governing parameters–and perhaps fundamentally different governing equations–than those with adequate resilience.

The Study of Physical Resilience and Aging (SPRING) is a study with high potential for

aiding resilience research. The study provides data on physiological systems with hypothesized relevance to resilience through measurements of cortisol, glucose, physical fatigability (reported fatigue after a standardized task), blood pressure, heart rate variability, and immune cell response (Walston et al., 2023). In some cases, explicit stimulus-response experiments were performed. In others, daily life was considered as the stressor, and monitoring was performed over the course of a day. A key challenge arose from the constraints of clinical research: For most measures, only 3-4 measurements including baseline and subsequent measures following stimulus were feasible to obtain. New questions arise—is it possible to estimate underlying governing equations if these are not known a priori, let alone with only four data points per person? The following paper addresses study design questions motivated by this question and the larger study. Through simulation studies, we assess the bias and precision of curve estimation using Local Linear Approximation (LLA) as the number of sampled points and amount of measurement error in the data collection change (Boker and Graham, 1998).

We specifically study LLA in order to estimate curves' governing equations. This choice was motivated by the SPRING study design, where the sparsity of serial sampling limits the complexity of procedure that can be applied. There is substantial literature surrounding LLA, but little has been published regarding its application to sparsely sampled time series. We aim to better understand the amount of sparseness and noise that renders local linear approximation inaccurate or imprecise for curve parameter estimation. We also aim to determine how accuracy and precision of parameter estimation differs as the frequency and damping of the true curve change. These findings will aid in identifying gaps in methodologies best suited for dynamical systems modeling of sparsely sampled data with appreciable measurement error.

This paper first provides background on dynamical systems and the estimation of differ-

ential equations governing their behavior from data. A methods section first describes the characteristics of the population curves from which we sample and attempt to estimate, then provides in-depth detail behind the simulation, from generating the data to estimating curves and assessing that estimation. The results section is organized into two main parts. The first part explores estimator properties when applied to data sampled from the true curves with no measurement error—we refer to this as "exact data" or data with "no noise" throughout the paper. The second part mirrors the previous; it explores estimator properties when applied to data sampled from the curves in the presence of measurement error with varied variability—referred to as "noisy data" or "data with noise" throughout this paper. Lastly, the discussion section ties in conclusions and foresees future work.

Identifying systems dynamics governing resilience would lay foundation for preventive and interventional treatments to increase resilience. It also might increase clinicians' ability to discriminate older adults capable of rebounding from stressful procedures from those at risk for long-term adverse consequences, thereby laying groundwork for improved clinical management strategies.

2. Methods

2.1 *Dynamical Systems*

Complex dynamical systems are at the center of the resilience hypothesis. In this context, a dynamical system is comprised of numerous components that interact with each other temporally and together result in one's physiological state and dynamics (Fried et al., 2021). The key is a focus not on each component individually, but on the system of interacting components. These components scale from the cellular and molecular level, such as mitochondria and proteins, to larger physiological systems, such as the musculo-skeletal, stress-response, and metabolic systems (Fried et al., 2005). Communication via feedback loops, protocols,

and other systematic functions are key to these dynamical systems, which Csete and Doyle argue are simultaneously robust and fragile (Csete and Doyle, 2002). Governing equations mathematically model the complex behaviors of these dynamical systems.

Physically resilient adults are hypothesized to have their multi-systems functioning harmoniously and efficiently (Varadhan et al., 2018). On the other hand, adults with low resilience are hypothesized to have critically dysregulated dynamical systems. This is expected to occur as individual systems decline, which leads communication and feedback between systems to deteriorate. Eventually, the dysregulation of the systems crosses a threshold and a state of low resilience emerges (Fried et al., 2021). In mathematical terms, we hypothesize that the complex dynamical systems for resilient and non-resilient adults are governed by distinct equations–either in form or parameters.

2.2 *Dynamical Systems*

In most cases to be studied in SPRING, the equations governing the dynamical systems are unknown. We therefore seek to learn them– at least approximately–empirically. To do this, we employ Local Linear Approximation, which we describe in a future section. LLA allows us to estimate curve derivatives and approximate underlying system dynamics using a simple second order linear differential equation (Equation 1). This differential equation is characteristic of a Damped Linear Oscillator (DLO) (Equation 2). Although we are not assuming the DLO most accurately models SPRING or any other biological data, we are motivated to pursue this more simplistic linear approximation by the sparsity of our data. Given more data, we would consider complex, nonlinear models. It is also important to note that we also generate our theoretical data using the DLO. We do this not because the DLO serves as a true model, but to acknowledge its connection to our methodology and assess the success of curve recovery in a controlled scenario.

The approach we pursue has precedent in related literature–LLA and the DLO has been

used in dynamical system applications across disciplines (see LLA section). A particularly relevant example is Ackerman and colleagues' use of a more complex form of the DLO (the Ackerman model) to approximate blood sugar following an oral glucose tolerance test (Ackerman et al., 1964). This glucose-tolerance test is a component of the SPRING study we wish to utilize in evaluating resilience status. Although the Ackerman model aligns with the context and goals of our setting, its complexity renders it a very difficult model–particularly in a sparse data scenario.

As mentioned, all data in this study are simulated using variations of a general equation for a damped linear oscillator shown in Equation 2 (Equations adapted from Boker & Graham, 1998).

$$\frac{d^2x}{dt^2} = \zeta\frac{dx}{dt} + \eta x. \tag{1}$$

$$x = Ae^{\frac{1}{2}\zeta t}cos\left(t\sqrt{-\eta - \frac{\zeta^2}{4}} + \phi\right). \tag{2}$$

The value of A controls the initial amplitude of the oscillation. ϕ controls the phase constant–the initial phase offset. The exponential term controls the damping of the system—the more negative the value of ζ, the greater the rate at which the amplitude decreases and the more damped the system is. The cosine term $\sqrt{-\eta - \frac{\zeta^2}{4}}$ controls the frequency– where η is the primary function of the frequency of the undamped oscillations: The more negative the value of η, the greater the frequency. We will refer to ζ as the damping parameter, and η as the frequency parameter. It is important to note this parameterization does not completely partition damping and frequency. However, this is standard notation in the literature. ζ and η are the two parameters of interest throughout this paper.

2.3 *LLA*

Local Linear Approximation is the methodology we study for estimating governing equations. LLA is a well-known method for fitting first and second order differential equations– it has a

long history of use to explore regulatory systems and system dynamics modeled by damped linear oscillators (Boker and Graham, 1998; Boker, 2001; Boker et al., 2010; Steele and Ferrer, 2011; Butner et al., 2005; Boker and Nesselroade, 2002). Variations of this methodology have also been developed and are explored in a future section.

This work uses LLA to estimate the first and second derivatives of the curves at each sampled point. These derivative estimations are then utilized in Equation 1 to estimate the damping and frequency parameters of the curves. We assume that all measurements are equally spaced.

First, *windows* of the data are created, which are subsets of the data containing some number of t-wise consecutive points. The size of the subsets (*window size*) determines which data are used to estimate derivatives at a single-location–the mid-point of the window. We consider window sizes of three and five points (henceforth referred to as three-point and five-point LLA). There is a trade-off between larger and smaller windows. Larger windows lead to broader summaries of curve behavior—these estimators may be less susceptible to noise but may not recover curve intricacies as well compared to smaller windows.

We assume each person j belongs to population i and has K total measurements. Thus, t_k denotes time-point k, $k = 1, ..., K$, and x_{ijk} denotes the value of x at time-point k for person j in population i. Detail and reasoning behind these enumerations will become more clear in a future section, but here we focus on LLA.

LLA works the same way for any window size, so we will explain in depth using the example of a three-point window size. The first window for person i in population j would comprise of $(t_{\mathbf{1}}, x_{ij\mathbf{1}})$, $(t_{\mathbf{2}}, x_{ij\mathbf{2}})$, and $(t_{\mathbf{3}}, x_{ij\mathbf{3}})$. For any window, there are three data-points of interest–those located at the start, the center, or the end point of the window. We will refer to these as $(t_{\mathbf{[k-1]}}, x_{ij\mathbf{[k-1]}})$, $(t_{\mathbf{k}}, x_{ij\mathbf{k}})$, and $(t_{\mathbf{[k+1]}}, x_{ij\mathbf{[k+1]}})$, respectively. Note that in five-point LLA, the indices would be [k-2], k, and [k+2]. Using these three points and the fact of equal

spacing, the first and second derivatives are calculated according to Equations 3 and 4. These calculated derivatives correspond to the midpoint, $(t_{\mathbf{k}}, x_{ij\mathbf{k}})$.

$$\widehat{\frac{dx}{dt}}_{ij\mathbf{k}} = \frac{x_{ij[\mathbf{k-1}]} - x_{ij[\mathbf{k+1}]}}{2(t_{\mathbf{k}} - t_{[\mathbf{k-1}]})}. \tag{3}$$

$$\widehat{\frac{d^2x}{dt^2}}_{ij\mathbf{k}} = \frac{x_{ij[\mathbf{k+1}]} - x_{ij\mathbf{k}}}{(t_{\mathbf{k}} - t_{[\mathbf{k-1}]})^2} - \frac{x_{ij\mathbf{k}} - x_{ij[\mathbf{k-1}]}}{(t_{\mathbf{k}} - t_{[\mathbf{k-1}]})^2}. \tag{4}$$

After these calculations are completed and stored, the window shifts forwards by one point. The next window in this example would comprise of $(t_{\mathbf{2}}, x_{ij\mathbf{2}}), (t_{\mathbf{3}}, x_{ij\mathbf{3}})$, and $(t_{\mathbf{4}}, x_{ij\mathbf{4}})$, and the process repeats. By the completion of three-point LLA, there is an estimated first and second derivative at every sampled point in the data, except for the first and last points. Five-point LLA utilizes less of the data, as the first two and last two points do not have estimated first and second derivatives.

2.4 *Other Methodologies for Estimating Governing Equations*

We considered other methodologies to model governing equations of dynamical systems, many of which are more complex than LLA. One noteworthy methodology is latent differential equation modeling (LDE)– an extension of LLA that utilizes time-delay embedding to estimate parameters in differential equation models (Boker and Laurenceau, 2006; Boker et al., 2004). Another is Bruton et. al's Sparse Identification of Nonlinear Dynamics (SINDy)– a generalization of LLA that can entertain equations more complex than the DLO and that has extensions ranging from experimentation with regression penalties to addressing sparse, noisy, or corrupted data (Brunton et al., 2016; Venkatraman et al., 2023; Cozad et al., 2014; Schaeffer and McCalla, 2017; Messenger and Bortz, 2021; Kaheman et al., 2022; Tran and Ward, 2017; Champion et al., 2020; Fasel et al., 2022). Other researchers have incorporated machine learning approaches, with equally vast extensions and methodologies (Lejarza and Baldea, 2022). It is also worth briefly addressing a third approach– Functional Data Analysis (FDA)– which frames longitudinal datum as curves instead of individual measurements.

Although its techniques relate to curve fitting, FDA does not explicitly focus on our interest of curve dynamics (Ramsay, 1982; Ramsay and Dalzell, 1991; James and Sugar, 2003; Yao et al., 2005; Thompson and Rosen, 2008).

There is clearly a vibrant and diverse field surrounding governing equations of dynamical systems. However, as the complexities of these methodologies grow, so does their inapplicability to our case of extremely sparse data. After considering this research, we ultimately opted to pursue the much simpler LLA procedure from which many of these ideas stem.

2.5 *Specifying Population-level Curves*

We generated two sets of four curves with distinct damping and frequencies in order to tease apart their effects on curve estimation. The first set of four curves, curves A1-A4, all share the same frequency parameter and differ in their damping parameters. We refer to these as *A Curves* throughout the paper. The second set of four curves, curves B1-B4, all share the same damping parameter and differ in their frequency parameters. We refer to these as *B Curves*.

Curve A1 has the most damping, followed by curves A2, A3, and A4. B curves share the same damping but differ in frequency. Curve B4 has the greatest frequency, followed by curves B3, B2, and lastly, B1. Table 1 lists the exact damping and frequency parameters of the eight true curves.

[Table 1 about here.]

2.6 *Simulating Data*

We created each curve to be characteristic of a distinct population, i, where $i = 1, ..., 8$. More specifically, each curve represents a population-level governing equation of some theoretical physiological system, such as the motivating example of glucose metabolism following an OGTT. These governing equations are represented using a variation of the Damped Linear

Oscillator given in Equation 5, where η_i and ζ_i are the distinct governing parameters for population i. Time is given by t, and the the measurement of some theoretical chemical or hormone is given by x.

We assumed 100 people are sampled from each population. We then simulated data for each person, j ($j = 1, ..., 100$), by sampling a pre-specified number, K, of points from that person's population-level curve. In the case of three-point windows, K ranges from 4 to 14; in the case of five-point windows, K ranges from 6 to 19.

Person-level data simulation required two stages. We first determined the time-points, t, at which x values were to be simulated for all people. To mirror the real-world scenario of limited budget and access to participants, we limited time-points of curve sampling to $0 \leqslant t \leqslant 7$. These values were picked as all eight curves complete close to one oscillation within this time-frame. The exact values of t were chosen such that the K time points were equally spaced between the values of 0 and 7.

The second step was to simulate the x values at those points. For a simulation with K sampled points, we denote t_k the k_{th} sampled time-point, where $k = 1, ..., K$. As previously mentioned, we denote x_{ijk} the value of x at t_k for person j from population i. The sampling equation is given in Equation 5.

$$x_{ijk} = e^{\frac{1}{2}\zeta_i t_k} cos\left(t_k\sqrt{-\eta_i - \frac{\zeta_i^2}{4}}\right) + \epsilon_{ijk}. \qquad \epsilon_{ijk} \overset{\text{iid}}{\sim} N(0, \sigma). \tag{5}$$

The σ term in Equation 5 reflects the amount of random measurement error and inter-individual variation within a population (noise). For each t_k, we simulated x_{ijk} both with and without any noise. To simulate x_{ijk} with noise, we sample i.i.d ϵ_{ijk} from a 0-centered normal distribution with a pre-specified standard deviation $0 < \sigma \leqslant 1.9$. This reflects the more realistic case where individual variation from the population and measurement error exist. To simulate x_{ijk} without noise, we set $\sigma = 0$. This reflects the purely theoretical case

of both perfect measurement and perfect individual adherence to the population level curve. In this case, all people within a population have identical data.

Throughout this paper we refer to the level of noise using the standard deviation of its distribution. For example, "noise with a standard deviation (SD) of 0.08" implies $\epsilon_{ijk} \overset{\text{iid}}{\sim} N(\mu = 0, \sigma = 0.08)$ and "increasing noise" implies increasing σ. Although we refer to σ in terms of its value, it is important to note its context in relation to the curve. The initial amplitude of all eight curves is 1, meaning a σ of 0.08 is 8% of the initial amplitude. As the curves are damped, this percentage becomes larger compared to later amplitudes–particularly for more damped curves.

All data was generated independently. This does not reflect a real world scenario and will be addressed in the discussion section. Besides this independence assumption, the structure of the simulated data mimics the structure of the motivating SPRING study. We have assumed each person has their data collected at K time points, which are equally spaced between the beginning and end of the sampling period. Furthermore, data are collected for all people within and between populations at the same time points. Given 100 people in a population and 4 time-points per person, there would be 100 measurements at each time-point and 400 measurements total for the population. Note that unlike in the SPRING study, we do not necessarily sample at the first and last points of the sampling period. Given the oscillating nature of the curve and relatively arbitrariness of our sampling period, this should not affect the conclusions.

2.7 *Procedure of Curve Estimation through Local Linear Approximation*

Each person had exactly K sampled data points. The derivative approximations through LLA were conducted within individuals, meaning no additional data across individuals was utilized for this step. This resulted in first and second derivative approximations corresponding to each internal (t_k, x_{ijk}) data point for that person (recall the first and last data points do not

have estimated derivatives for three-point LLA, and the first and last two data points do not have estimated derivatives for five-point LLA).

Focusing on the example of three-point LLA, each person had $(K-2)$ distinct datum of the form $(t_k, x_{ijk}, \frac{\hat{dx}}{dt}_{ijk}, \frac{\hat{d^2x}}{dt^2}_{ijk})$ following LLA. Next, this person-level data was pooled within each population to create one dataset. For a population with 100 people, there was a total of $100\times(K-2)$ data points in the dataset. The linear regression outlined in Equation 1 was performed on this dataset to estimate population-level parameters η_i and ζ_i.

It is important to again note the implications of using i.i.d data. We did not account for correlation within each person's data or between windows; further remarks on this choice follow in the discussion.

2.8 *Large Scale Simulations*

2.8.1 *Simulating data over increasing numbers of sampled points.* Multiple large simulations were conducted on all eight curves (curve parameters in Table 1). The first set held noise constant with a standard deviation of either 0 (no noise) or of 0.08 as the number of sampled points per person increased at 1-point increments from 4 to 14 for three-point LLA or from 6 to 19 for five-point LLA. The value of 0.08 SD was chosen as it introduced considerable noise without rendering the curves unrecoverable. A visualization of underlying curves overlaid with sampled points having 0.08, 0.3, and 0.5 standard deviations of noise present is given in the supplement (Figure A.1).

2.8.2 *Simulating data over increasing levels of measurement variation.* The second set of simulations held the number of sampled points per person constant at either the lowest possible value for LLA (4 points for three-point LLA or 6 points for five-point LLA) or at 25 sampled points per person as the SD of the noise term increased from 0 to 1.9 at 0.1 increments. The values of 4 and 6 points were selected as both result in two distinct points with estimated derivatives per person after three-and five-point LLA. 25 points was chosen

as it was a large enough number to represent a more heavily sampled curve, while still being at the limit of clinical feasibility.

2.8.3 *Simulating data over increasing LLA window size.* A set of third simulations was performed to briefly address the impact of LLA window size on estimation. We sampled 25 points per curve with noise standard deviation at 0, 0.08, or 0.6. For each noise and point combination, we increased the window size from 3 to 19 points at intervals of 2 points. For all above simulations, 100 replicates at each unique noise level, number of sampled points, and LLA window size combination were performed.

2.9 *Analysis of Curve Estimation*

For each batch of replicates, the accuracy and precision of curve parameter estimators were assessed using bias, Mean Squared Error (MSE), empirical Standard Error (SE), and the Integrated Squared Difference (ISD) between the overall true and estimated curves. Equation 6 gives the calculation for the ISD, which is the difference between the true curve and the estimated curve squared and integrated between the x-range endpoints of 0 and 7. We also plotted estimated curves with the true curves for visual assessment.

$$ISD = \int_0^7 \left[e^{\frac{1}{2}\zeta_i t} cos\left(t\sqrt{-\eta_i - \frac{\zeta_i^2}{4}} \right) - e^{\frac{1}{2}\widehat{\zeta}_i t} cos\left(t\sqrt{-\widehat{\eta}_i - \frac{\widehat{\zeta}_i^2}{4}} \right) \right]^2 dt. \tag{6}$$

Note that for clarity and concision we do not include the MSE results directly in this paper. However, figures and additional text are located in the supplement (B.1, B.3, C.3, C.9, D.1).

3. Results

The key results are presented in two parts. First, we report the case of increasing numbers of sampled points and fixed measurement error. Second, we report the case of increasing measurement error and a fixed number of sampled points. We report these results primarily of three-point LLA, with a secondary focus on five-point LLA. Within each part, we first assess

high-level success of curve estimation through visualizations of estimated curves against true curves and through ISD. We follow this with analyses of parameter estimator bias and precision. Note that since each population contains 100 sampled people, "4 points per person" is equivalent to "400 points per curve" or "population". Following these key sections, we briefly address increasing window size and fixed sampled points and measurement error.

It is important to briefly comment on the language we use to describe curve fit. Recall that more negative damping and frequency parameters correspond to greater amounts of damping and frequency in the curve, respectively. Throughout this paper we will comment on the over/underestimation of the damping and frequency *of the curve* (where overestimation implies there is too much frequency or damping present, and underestimation implies there is too little), as opposed to the over/underestimation of the damping and frequency *parameters*.

We speculate that curves with greater damping more closely model dynamical systems of more resilient populations, whereas curves with less damping more closely model those of less resilient populations. There is less of an intuitive relationship between the frequency parameter of a curve and resilience level of the population it models, but this characteristic of the curve is still of great interest.

3.1 *Increasing Number of Points Sampled with Fixed Measurement Error*

3.1.1 *Visualizations of Estimated Curves.* For both noise standard deviations of 0 and 0.08, the curves estimated with 400 sampled points (4 points per person) had more damping and much lower frequencies than the true curve (Figure 1). For all curves, the estimated peaks and nadirs occurred at greater t values and were shallower than the true values. This trend was amplified under sampling conditions with error compared to no error. However, curves estimated using 600 and greater sampled points were similar under conditions with and without error. As the number of points used to estimate the curve increased, the estimated curve's damping became accurate more quickly than its frequency. Curves with lower true

frequencies, such as curve B1, were more accurately estimated at fewer sampled points compared to their higher frequency counterparts. These trends were similar across all eight curves.

Overall, qualitatively reasonable estimation was achieved for as few as six sampled points using three-point LLA. Five-point LLA required significantly more points for such reasonable estimation– Figures C.5 and C.6 in the supplement demonstrate that even at 12 points sampled per person, the true curve had not been well estimated.

[Figure 1 about here.]

3.1.2 *Accuracy.* Figure 2 depicts bias and ISD of the estimated curves. In the exact sampling case, the curves' damping and frequencies were underestimated for all eight curves, which corresponds to an overestimation of these two parameters. This underestimation of damping was most severe for more damped curves but unaffected by curve frequencies. Similarly, the underestimation of frequency was most severe for curves with greater frequencies but unaffected by a curve's damping. In all cases, damping and frequency bias decayed exponentially to 0 as more points were sampled. Five-point LLA exhibited the same trend but with slightly higher overall bias (Figure C.1 in supplement).

Under sampling conditions with error, the frequency of the true curve had an impact on damping estimation, which was not true in the exact sampling case. The converse was also somewhat true at greater sampled points–damping had a small impact on frequency estimation. For all curves at few points, damping was overestimated and frequency was underestimated (corresponding with underestimated damping parameters and overestimated frequency parameters). As points increased, both curve characteristics became more accurate, then began to be overestimated. The greater the damping or the lower the frequency of the true curve, the greater the extent of damping and frequency overestimation. Five-point LLA differed in the extent of overestimation– the amount of damping was almost never

overestimated, and frequency was to a lesser extent. The other trends were comparable between three-point and five-point LLA.

As the number of sampled points grew, the ISD decreased to $\tilde{0}$ for all curves (Figure 2). Curves with the highest frequencies and least damping had the highest ISD values, but this difference shrunk as more points were sampled. The elbows of the ISD plots were at approximately 6 points per person (± 1 point per person). This suggests this number of sampled points was a turning-point for goodness of the curve fit, which aligns with previous observations. Interestingly, the ISD values for all curves were similar between the sampling scenarios with and without noise. Five-point LLA showed comparable trends, but had slightly higher ISD values overall (Figure C.2 in supplement)

Overall, curve recovery was relatively successful despite some parameter bias. This may reflect not only the estimability of parameters in this design, but also its ability to identify the two parameters from one another. Particularly without noise present, these results were promising.

[Figure 2 about here.]

3.1.3 *Precision.* For curves estimated from points sampled with no noise, there is no variance over the 100 iterations of the simulation at each point by design. We will not assess standard error or MSE for this case.

For curves estimated with noise present, all curves shared similar trends in standard error of damping parameter estimates (Figure B.2 in supplement). As expected, almost all eight curves reached their maximum SE at 4 points per person. This peak varied by curve, but all A curves ranged between peak values of $\sim$0.06 and 0.08, whereas B curves ranged between $\sim$0.02 to 0.06. As sampled points increased past five points per person, the damping standard errors of the curves hovered around 0.01, where curves with more damping asymptoted at

slightly higher standard errors. Evidence of this trend can be seen in the decreasing IQRs of the boxplots in Figure 2.

The SE of frequency parameter estimates showed a different trend. Although all curves also reached a local maximum SE value at 4 points per person, the SE of frequency estimates increased overall linearly as sampled points increase. However, this occurred at a smaller scale– the SE ranged from 0 to 0.03 for all curves. Curves with greater damping tended to have higher SE values for both parameter estimates, whereas there was no clear trend in variation with increasing frequency.

3.2 *Increasing Noise over Fixed Number of Sampled Points*

3.2.1 *Visualizations of Estimated Curves.* Figure 3 demonstrates none of the eight curves estimated using 4 or 25 points per person with at least 0.1 standard deviations of noise captured the true curve's behavior. Curves estimated from both 4 and 25 points tended to overestimate the damping at low noise values and underestimate it at high noise values. However, 4-point estimated curves had underestimated frequencies and 25-point curves had vastly overestimated frequencies. The extent of over or underestimation in these characteristics grew with the noise SD. Five point LLA was comparable, but this frequency overestimation was less extreme (Figures C.11, C.12 in supplement)

[Figure 3 about here.]

3.2.2 *Accuracy.* For all 25-point estimated curves, initial increases in noise corresponded to bias in the estimated damping parameter that first briefly dipped to negative values before increasing to positive values (4). This meant the curves' estimated damping moved from relatively accurate, to overestimated, back to relatively accurate, and finally to underestimated. The curves' estimated frequencies under 25-point sampling did not share this fluctuation in bias–the curve frequency was overestimated (i.e frequency parameters underestimated) as

soon as noise was introduced, and then it continued to be increasingly overestimated before the bias reached an asymptote around -20 for all curves. Estimates of more damped curves had more extreme frequency and damping bias. Damping bias was unrelated to the frequency of underlying curves, but curves with lower frequency exhibited more extreme frequency bias.

Bias in estimated damping was similar in 4-point curves as it was in 25 point curves, although the overestimation was not as extreme. On the other hand, the frequency bias in the 4-point case was dissimilar to that of the 25-point case. The scale for 4-point estimates was much smaller ($\sim \frac{1}{10}$ of the range), and the curves' frequencies were consistently underestimated instead of overestimated. This bias was most extreme for true curves with greater frequency and, to a lesser extent, curves with more damping. Five-point LLA showed again similar trends. The main difference was its lower frequency bias in the 25-point case (Figure C.7 in supplement)

Overall, the ISD increased with the noise standard deviation (4). Interestingly, the ISD was slightly higher overall for the 25-point sampling case compared to the 4-point sampling case, particularly at higher noise SD values. Curves with less damping had greater ISD values for both 25 and 4-point sampling scenarios than curves with more damping. Compared with higher frequency curves, curves with lower frequencies had slightly lower ISD values under the 4-point sampling case, but nearly identical ISD values under the 25-point sampling case. Thus, damping had an impact on ISD regardless of the number of points sampled, whereas frequency only made a difference in cases of lower sampled points.

Another interesting observation was the difference in ISD at low noise levels. Under 4 sampled points, the ISD was greater than 0 when no noise was present, indicating the issue in curve estimation here lay with its few sampled points. Under 25 sampled points, the ISD started at 0 for all curves but the value for A curves quickly grew as noise SD reached 0.3.

The ISD under five-point LLA was slightly lower overall under its 6-point sampling case, but otherwise comparable (Figure C.8 in supplement).

[Figure 4 about here.]

3.2.3 *Precision.* For all 4-point estimated curves, standard errors for frequency and damping estimates abruptly increased to an approximate plateau as noise was introduced (Figure B.4 in supplement). Whereas the SE values for most curves had reached their plateau when noise was at 0.1 SD, it took more noise ($\sim$1.2 SD) for less damped curves to reach the frequency SE plateau of $\sim$0.03, and for lower frequency curves to reach the damping SE plateau of $\sim$0.06. These plateaus implied that despite growing noise, the variation of the estimators stayed relatively constant.

All 25-point estimated curves required higher noise levels for the SE values of frequency and damping estimates to begin leveling off, which occurred around SE values 0.5 and 0.05, respectively. A key difference between this and the 4-point case was the presence of global trends in SE even after the rate of change had slowed significantly. As noise continued to grow, there was a slight overall decrease in the SE of the damping estimates and an overall increase in that of the frequency estimates.

Five-point LLA had similar trends as three-point LLA, though its values were slightly lower and the aforementioned global trends were not as apparent (Figure C.10 in supplement).

3.3 *Increasing Window Size over Fixed Noise and Sampled Points*

Under perfect measurement of 25 points per person, smaller window sizes resulted in less biased measurements and smaller mean squared errors– both values were close to 0 for damping and frequency parameter prediction at three-points per window. As window size increased, both the damping and frequency of the curve became underestimated. The bias was more extreme for more damped and higher frequency curves.

Once noise SD increased to 0.08, the optimal window size increased to five-points per window– all bias, ISD, and MSE values were closest to 0 under this condition. There was some oscillation in the damping parameter bias for more damped or higher frequency curves, and higher frequency curves also had more biased frequency estimations.

At a higher noise value of 0.6 SD, the optimal window size was more complex. Whereas the curve frequency was extremely overestimated under a three-point window (bias < -10), it achieved near-perfect frequency estimation under a seven-point window. As window size continued to increase, the frequency became consistently underestimated. Unlike frequency, the curves' damping was estimated most accurately at three-point windows for more damped curves. The damping of less damped curves was slightly overestimated at three-point windows and slightly underestimated for all larger windows. Despite discrepancies between ideal window sizes for damping and frequency estimation, the ISD reached its minimum ($\sim$0.5) for almost all curves at seven or nine point windows.

4. Discussion

We attempted to recover parameters of simulated governing equations under conditions of varying sparsity, noise, and window size using LLA and known properties of the damped linear oscillator. Because of the motivating issue of sparsity, we primarily considered three-and-five point windows for simulations, which are the focus of discussion. It is clear that care is needed in utilizing this technique of LLA for uncovering governing curve dynamics. Although broadly robust under specific conditions ($>$ 6 sampled points/person with no noise or 10-12 sampled points/person with low noise in these simulations), this technique fails when variation or sparsity is introduced absent a meticulous tailoring of window size, which may be infeasible in sparse sampling scenarios.

Past a certain threshold of noise, all curves were estimated to have no damping and a shared frequency parameter ($\sim$-0.4 when 4 points were sampled or of $\sim$22 when 25 points

per person were sampled under three-point LLA). Presence of noise was a major issue under all simulations, but there were still differences in impact– for example when 25 points were sampled per person, appreciable noise caused more extreme frequency overestimation under three-point LLA compared with five-point LLA. This highlights the importance of thoughtful window-size selection in addressing noise.

The problem of sparsely sampled data also had consequences– albeit less severe consequences than that of unaddressed noise. Unsurprisingly, curve recovery was generally unsuccessful at the lowest numbers of sampled points, even when noise was minimal-to-none. When noise was present, sampling both too few and too many points led to bias in opposite directions. This suggests more measurements are not necessarily better and a Goldilocks range of accurate estimation may exist. The range for these simulations was approximately 9-11 points per person, but this is specific to the true curve parameters, noise present, and window length. Finally, initial small increases in the number of sampled points had a large impact on the accuracy of curve estimation, implying just one or two more measurements per person makes a significant difference in later interpretation.

The precision analyses produced additional insight. The standard errors of parameter estimations plateaued as noise increased in the case of 4-points sampled per person, supporting the prior observation that beyond a certain threshold of noise, the performance of the LLA procedure and results showed little change as noise continued to increase. An interesting difference is with the case of 25-points sampled per person, in which standard errors for frequency parameter estimation continued to increase with increasing noise. This in tandem with the increasing SE of frequency (and less so, damping) estimation at high numbers of sampled points add to this picture of volatility in estimation (particularly, frequency estimation) in the case of high sampling frequency coupled with substantial noise.

Overall, both frequency and damping estimators were less accurate for more damped

curves. Generally, the degree of damping of the true curves tended to have an impact on the accuracy of frequency parameter estimation, but the converse was not always true. There was less of a single and clear trend in the effect of true frequency on accuracy or precision of frequency parameter estimation.

We acknowledge limitations with our work. One is our use of independently generated data. As briefly mentioned, this would not be the case in any real-world scenario. This allowed us to work with simpler relationships between points, windows, and simpler regressions, but future work is needed to address dependence in data. We also only studied the case of equally-spaced measurements. Randomly-spaced measurements unique to each participant might better support a priori smoothing, which would open up other possibilities for estimating derivatives. We leave this as more future work that could also inform sampling design or alternative methodology.

A final limitation is our usage of the DLO to generate our data. Real-world biological data may not be so well approximated with this model. Regardless, this usage of the DLO has ample precedent, with Boker & Graham and Steele & Ferrer reporting the DLO to be a flexible model that adequately fit their non-simulated data. Although we can't speak on applications to real data (yet), we did find some robustness to this technique in the context of no or little noise and an adequate number of sampled points. The DLO was also beneficial in its simplicity and flexibility. This allowed us to explore the impact of frequency and damping parameters on curve recovery in-depth.

To lastly put this work in further context, our findings aligned with previous literature on certain key observations. Boker and Graham found the interval of time between measurements an important factor in determining the level of bias present in parameter estimates– a factor researchers should try to optimize (see Boker and Graham 1998 for this methodology). In their 2002 paper, Boker and Nesselroade added insight on spacing. They

found that when time between observations was short, added noise had more of an impact on parameter bias. Although we focused on window size instead of data spacing and density, the concepts are inherently linked. We similarly observed that the choice of LLA window size is central to optimal estimation– as noise increases, larger window sizes become generally more desirable with their smoother-like properties. Smaller window sizes pick up on more nuance–including measurement error or individual variations–which makes population-level estimation difficult. In our data, this resulted in overestimated frequencies (although the damping estimation was less affected). Proper choice of window size is thus key in utilizing LLA. However, window size options are extremely limited in the case of sparse data.

Our work also supported previous conclusions that LLA estimates can be relatively accurate given enough sampled points, although we further explored its limitations in the context of noise. Furthermore, we also found the frequency parameter generally more difficult to estimate than the damping parameter (Boker and Graham, 1998; Boker and Nesselroade, 2002)

Our work also adds novelty through some departure from previous findings. Boker and Nesselroade's 2002 paper attempted recovering DLO parameters with only three measurements per participant. They concluded that this technique relatively accurately recovered curve parameters in this sparse-data scenario. We did not find this to be the case– we were unable to recover the curve in the context of sparse data even in a low-to-no noise scenario, let alone under conditions of moderate noise. Despite this similar goal, the aim of their work also differed from ours. They explored both LLA and state-space embedding techniques in the context of asynchronous curve phases and varying measurement intervals, whereas we explored thorough design-based questions about LLA and the DLO in the context of sparsely sampled curves with noise present, the characteristics of the curves LLA most successfully recovers, and the limitations of LLA.

Considering these severe impacts of sparsity and, in particular, noise, this paper serves as a cautionary tale. Along with raising questions, it also adds to existing dialogue in exploring how curve characteristics and window size impact curve recovery. Future work is needed to either develop methodologies that can successfully perform this task without requiring ample and/or low-noise data, or to define limitations when these tasks are not possible. Future work is also needed to explore how to best design and leverage data collection when that collection is limited– for example, sampling at the most informative locations of the curve (ex: valleys, peaks).

These findings also shed light on resilience analysis in the context of SPRING. Both noisiness and low data interfered with differentiation between curves and thus potential classification of distinct populations. A protocol for dealing with any excess noise in the data is needed for LLA to be viable. Similarly, research is needed to assess levels of variation coming from individual versus population level differences, and how these are obscured by the amount of noise present. This will be a crucial future stage of research– attempting to cluster individuals by their governing equations to identify resilience sub-populations. We look forward to future discussion.

Acknowledgement We thank the Editor, Associate Editor, and referees for their valuable comments. We thank Dr. Howard Hu, Chair and Professor of Population and Public Health Sciences, Keck School of Medicine, University of Southern California, for his support for the bone lead data in the NAS. This research was partially supported by NIH grant CA129102.

FUNDING This research was partially supported by National Institutes of Health (NIH) grant CA129102 to Taylor.

CONFLICT OF INTEREST None declared.

DATA AVAILABILITY The data that support the findings in this paper cannot be shared publicly for the privacy of individuals that participated in the study.

PREPRINT STATUS: This work has not been peer reviewed.

References

Ackerman, E., Rosevear, J. W., and McGuckin, W. F. (1964). A mathematical model of the glucose-tolerance test. *Physics in Medicine and Biology* **9,** 203–213.

Boker, S. M. (2001). *Differential structural equation modeling of intraindividual variability*, pages 3–28. American Psychological Association.

Boker, S. M., Deboeck, P. R., Edler, C., and Keel, P. K. (2010). *Generalized local linear approximation of derivatives from time series.*, page 161–178. Routledge.

Boker, S. M. and Graham, J. (1998). A dynamical systems analysis of adolescent substance abuse. *Multivariate Behavioral Research* **4,** 479–507.

Boker, S. M. and Laurenceau, J.-P. (2006). *Dynamical systems modeling: An application to the regulation of intimacy and disclosure in marriage*, page 195–218. Oxford University Press.

Boker, S. M., Neale, M., and Rausch, J. (2004). *Latent differential equation modeling with multivariate multi-occasion indicators*, pages 151–174. Springer Netherlands.

Boker, S. M. and Nesselroade, J. R. (2002). A method for modeling the intrinsic dynamics of intraindividual variability: Recovering the parameters of simulated oscillators in multi-wave panel data. *Multivariate Behavioral Research* **37,** 127–160.

Brunton, S. L., Proctor, J. L., and Kutz, J. N. (2016). Discovering governing equations from data by sparse identification of nonlinear dynamical systems. *Proceedings of the National Academy of Sciences of the United States of America* **113,** 3932–3937.

Butner, J., Amazeen, P., and Mulvey, G. (2005). Multilevel modeling of two cyclical processes: Extending differential structural equation modeling to nonlinear coupled systems. *Psychological Methods* **10,** 159–77.

Champion, K., Zheng, P., Aravkin, A. Y., Brunton, S. L., and Kutz, J. N. (2020). A unified sparse optimization framework to learn parsimonious physics-informed models from data. *IEEE Access* **8,**.

Cozad, A., Sahinidis, N. V., and Miller, D. C. (2014). Learning surrogate models for simulation-based optimization. *AIChE* **60,** 2211–2227.

Csete, M. E. and Doyle, J. C. (2002). Reverse engineering of biological complexity. *Science* **295,** 1664–1669.

Fasel, U., Kutz, J. N., Brunton, B. W., and Brunton, S. L. (2022). Ensemble-sindy: Robust sparse model discovery in the low-data, high-noise limit, with active learning and control. *Proceedings of the Royal Society A* **478,**.

Fried, L. P., Cohen, A. A., Xue, Q., Walston, J., Bandeen-Roche, K., and Varadhan, R. (2021). The physical frailty syndrome as a transition from homeostatic symphony to cacophony. *Nature Aging* **1,** 36–46.

Fried, L. P., Hadley, E. C., Walston, J. D., Newman, A. B., Guralnik, J. M., Studenski, S., Harris, T. B., Ershler, W. B., and Ferrucci, L. (2005). From bedside to bench: research agenda for frailty. *Science of Aging Knowledge Environment* **2005,**.

Hadley, E. C., Kuchel, G. A., Newman, A. B., Allore, H., Bartley, J., Bergeman, C., Blinov, M., Colon-Emeric, C., Dabhar, F., Dugan, L., Dutta, C., Eldadah, B., Ferrucci, L., Kirkland, J., Kritchevsky, S., Lipsitz, L., Nadkarni, N., Reed, M., Schmader, K., and Yung, R. (2018). Report: Nia workshop on measures of physiologic resiliencies in human aging. *The Journals of Gerontology* **73,**.

James, G. M. and Sugar, C. A. (2003). Clustering for sparsely sampled functional data. *Journal of the American Statistical Association* **98,** 397–408.

Kaheman, K., Brunton, S. L., and Kutz, J. N. (2022). Automatic differentiation to simultaneously identify nonlinear dynamics and extract noise probability distributions

from data. *Science and Technology* **3,**.

Lejarza, F. and Baldea, M. (2022). Data-driven discovery of the governing equations of dynamical systems via moving horizon optimization. *Scientific Reports* **12,**.

Messenger, D. A. and Bortz, D. M. (2021). Weak sindy: Galerkin-based data-driven model selection. *Multiscale Modeling and Simulation* **19,** 1474–1497.

Ramsay, J. O. (1982). When the data are functions. *Psychometrika* **47,** 379–396.

Ramsay, J. O. and Dalzell, C. J. (1991). Some tools for functional data analysis. *Journal of the Royal Statistical Society* **53,** 539–561.

Schaeffer, H. and McCalla, S. G. (2017). Sparse model selection via integral terms. *Physical Review E* **96,**.

Steele, J. S. and Ferrer, E. (2011). Latent differential equation modeling of self-regulatory and coregulatory affective processes. *Multivariate Behavioral Research* **46,** 956–984.

Thompson, W. K. and Rosen, O. (2008). A bayesian model for sparse functional data. *Biometrics* **64,** 54–63.

Tran, G. and Ward, R. (2017). Exact recovery of chaotic systems from highly corrupted data. *Multiscale Modeling and Simulation* **15,** 1108–1129.

Varadhan, R., Walston, J. D., and Bandeen-Roche, K. (2018). Can a link be found between physical resilience and frailty in older adults by studying dynamical systems? *Journal of the American Geriatrics Society* **66,** 1455–1458.

Venkatraman, S., Basu, S., and Wells, M. (2023). Sparse reconstruction of ordinary differential equations with inference.

Walston, J., Varadhan, R., Xue, Q., Buta, B., Sieber, F., Oni, J., Imus, P., Crews, D. C., Artz, A., Schrack, J., Kalyani, R. R., Abadir, P., Carlson, M., Hladek, M., McAdams-DeMarco, M., Jones, R., Johnson, A., Shafi, T., Newman, A. B., and Bandeen-Roche, K. (2023). A study of physical resilience and aging (spring): Conceptual framework,

rationale, and study design. *Journal of the American Geriatrics Society* **71,** 2393–2405.

Yao, F., Müller, H. G., and Wang, J. L. (2005). Functional data analysis for sparse longitudinal data. *Journal of the American Statistical Association* **100,** 577–590.

Acknowledgements

Supporting Information

Received Month 2024. *Revised Month* Year. *Accepted Month* Year.

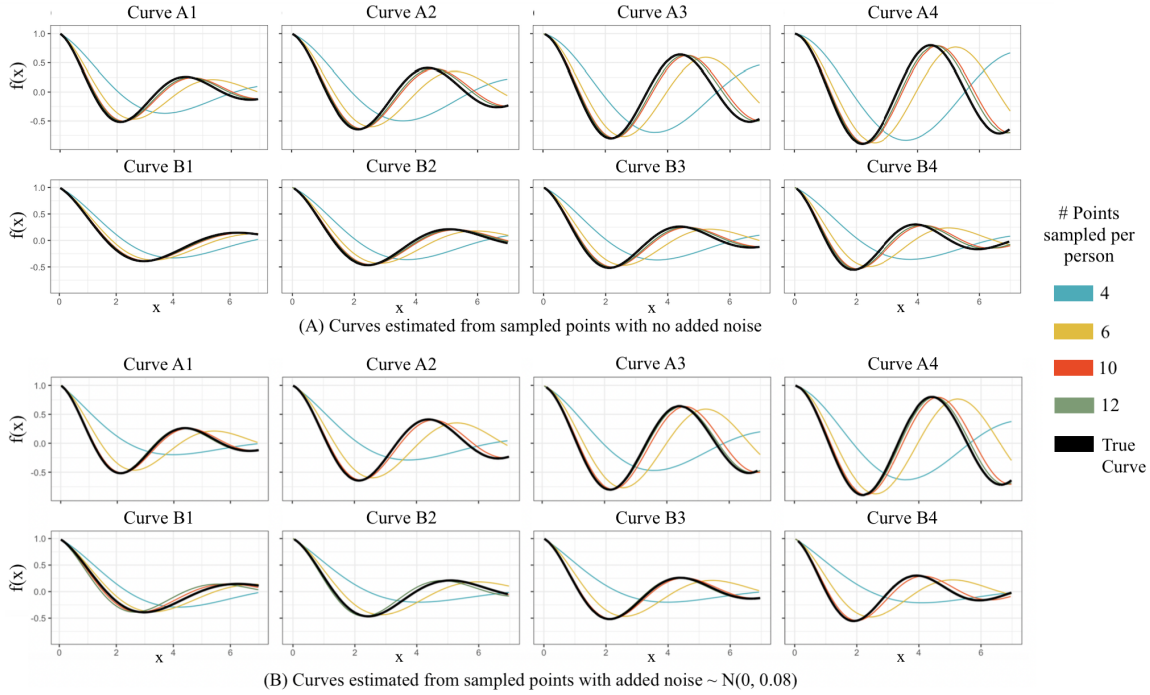

Figure 1. Each plot displays one the eight true curves (black) and its corresponding curves estimated using three-point LLA across 4, 6, 10, or 12 points per person (blue, yellow, red, green). In sub-figure (A) no noise was added to points. In sub-figure (B) noise drawn from N(0, 0.08) was added to the points.

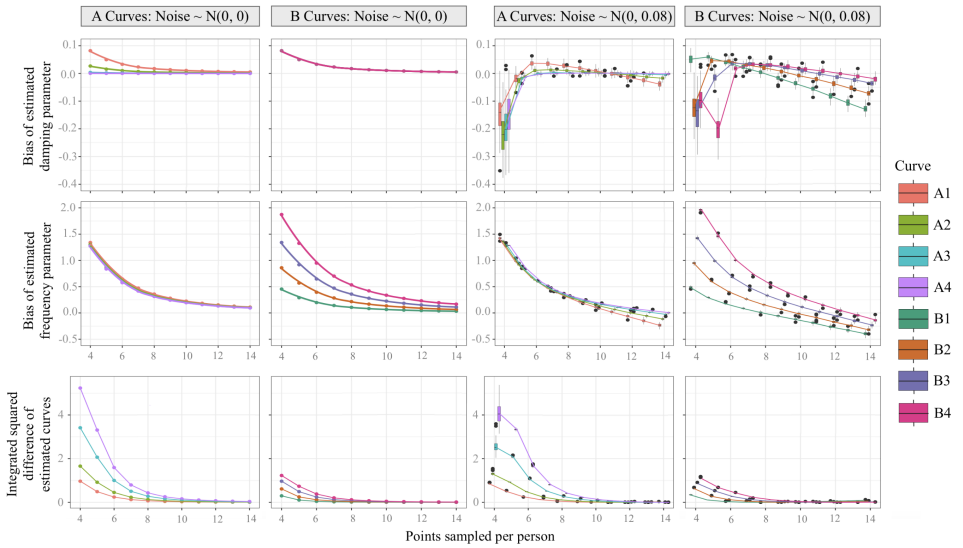

Figure 2. 12 sub-figures depict distributions of accuracy metrics of the 8 estimated curves as the number of sampled points/person increases. The first row depicts the bias of each estimated curve's damping parameter, the second row depicts the bias of its estimated frequency parameter, and the third row depicts the ISD between the estimated and true curve. Plots in the first and second column evaluate curve estimations from points with no noise added. Plots in the third and fourth columns evaluate curve estimations from points sampled with added noise $\sim$ N(0, 0.08). The first and third columns display A curves, and the second and fourth display B curves.

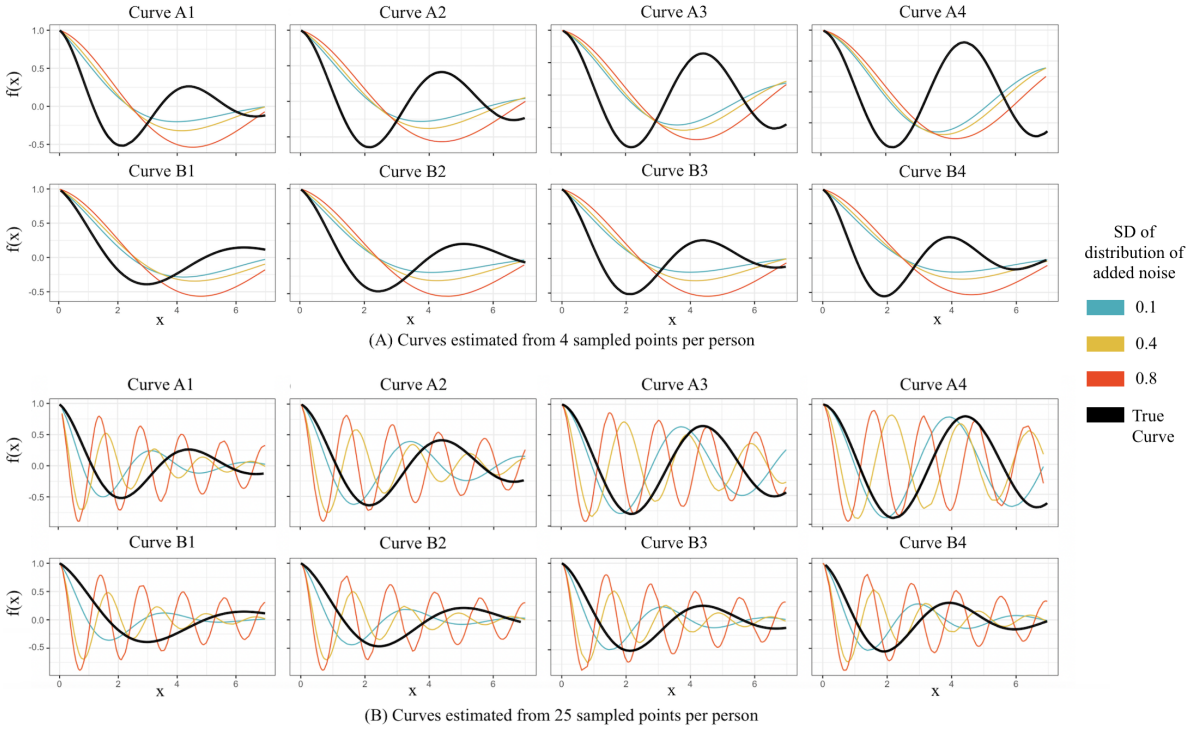

Figure 3. Each plot displays one the eight true curves (black) and its corresponding curves estimated using three-point LLA on points with added noise. The standard deviation of the added-noise distribution is 0.1, 0.4, and 0.8 for blue, yellow, and red curves, respectively. In sub-figure (A) 4 point were sampled per person. In sub-figure (B) 25 points were sampled per person.

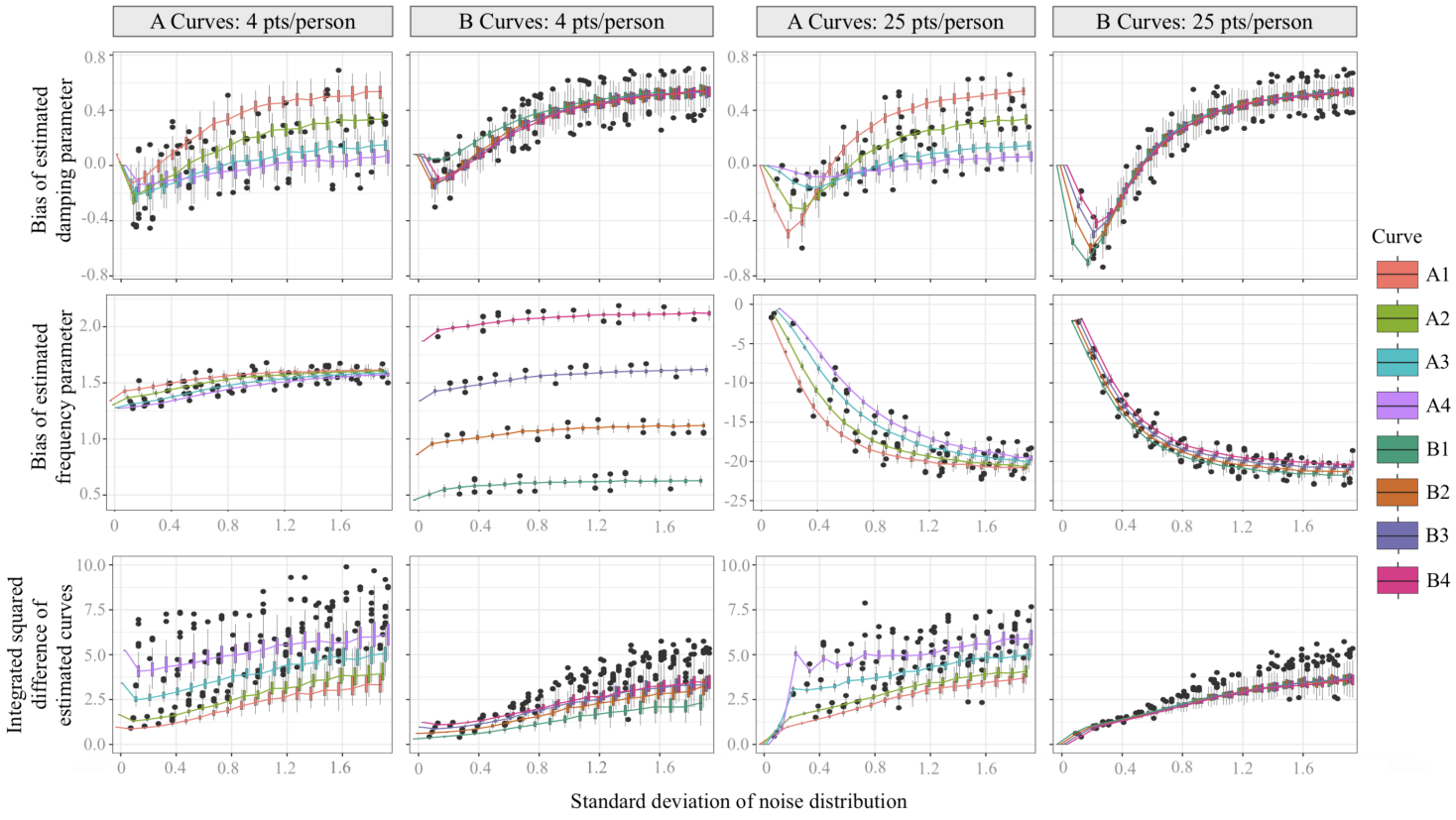

Figure 4. 12 sub-figures depict distributions of accuracy metrics of the 8 estimated curves as the standard deviation of the noise distribution increases. The first row depicts the bias of each estimated curve's damping parameter, the second row depicts the bias of its estimated frequency parameter, and the third row depicts the ISD between the estimated and true curve. Plots in the first and second column evaluate curve estimations from 4 points/person. Plots in the third and fourth columns evaluate curve estimations from 25 points/person. The first and third columns display A curves, and the second and fourth display B curves.

Curve	A	ϕ	ζ	η
A1	1	0	-0.6	-2.0
A2	1	0	-0.4	-2.0
A3	1	0	-0.2	-2.0
A4	1	0	-0.1	-2.0
B1	1	0	-0.6	-1.0
B2	1	0	-0.6	-1.5
B3	1	0	-0.6	-2.0
B4	1	0	-0.6	-2.5

Table 1
The labels and true parameters of the eight damped linear oscillator curves estimated throughout this paper
.